2010 American Control Conference
Marriott Waterfront, Baltimore, MD, USA
June 30-July 02, 2010

Sensor-Only Fault Detection Using Pseudo Transfer Function Identification

Adam J. Brzezinski[1], Sunil Kukreja[2], Jun Ni[3], Dennis S. Bernstein[4]

***Abstract*— Motivated by passive health monitoring applications, we consider identification where only sensor measurements are available. The goal is to exploit unknown ambient disturbances and thus avoid the need for controlled actuation. To achieve this, we identify a pseudo transfer function (PTF) between sensor measurements. For the single-input case, one sensor is designated as the pseudo input to the system, while the second sensor measurements constitute the pseudo output. We show that the identified PTF is independent of the unknown initial state and unknown exogenous input. We demonstrate this method on two- and three-degree-of-freedom mass-spring-damper systems and validate the identified PTFs by comparing them with analytical results.**

I. INTRODUCTION

In many applications of system identification, the system is driven by external signals that are not measured. In this situation, blind identification techniques can be used to obtain estimates of the system dynamics [1], [2]. Also, frequency-domain [3] and subspace-based [4] system identification techniques have been applied. Since the input signal is unknown, its statistical properties are usually assumed to be known in order to compensate for lack of knowledge of its time history.

In the present paper we develop an identification technique that uses multiple sensors but does not require measurements of or assumptions about the statistical properties of the external signal. We designate a subset of the sensor signals as the pseudo input(s) and another subset as the pseudo output(s). The resulting *pseudo transfer function* (PTF) from the pseudo input(s) to the pseudo output thus provides a map between the sensor signals.

The use of PTFs was introduced in [5] for the case of 2 sensors. In the present paper we extend this technique to $m \geq 2$ sensors, and we extend the theoretical foundation by providing detailed identities that allow us to reduce the order of the PTFs despite unknown nonzero initial conditions. We also investigate how sensor noise affects PTF identification.

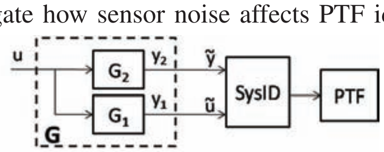

Fig. 1. Method for identifying pseudo transfer functions (PTFs).

To illustrate the notion of a PTF, consider the system in Figure 1, which has one input u and two outputs y_1 and y_2. To account for the initial state and resulting transient response, we cast the dynamics in terms of the forward shift operator $\mathbf{q}$, which yields

$$\delta(\mathbf{q})y_i = \eta_i(\mathbf{q})u, \tag{1}$$

where $\delta(\mathbf{q})$, $\eta_1(\mathbf{q})$, and $\eta_2(\mathbf{q})$ are polynomials in $\mathbf{q}$, and y_1, y_2, and u denote time sequences, that is, $y_1 = \{y_1(0), y_1(1), \ldots\}$, and $\mathbf{q}y_1 = \{y_1(1), y_1(2), \ldots\}$. For convenience, we can rewrite (1) in the transfer function form

$$y_i = G_i(\mathbf{q})u = \frac{\eta_i(\mathbf{q})}{\delta(\mathbf{q})}u, \tag{2}$$

although we stress that (2) represents the difference equation (1) rather than a relation between z-transforms, which play no role in this paper.

It follows from (1) that

$$\eta_2(\mathbf{q})\delta(\mathbf{q})y_1 = \eta_2(\mathbf{q})\eta_1(\mathbf{q})u, \tag{3}$$

$$\eta_1(\mathbf{q})\delta(\mathbf{q})y_2 = \eta_1(\mathbf{q})\eta_2(\mathbf{q})u, \tag{4}$$

and thus

$$\eta_2(\mathbf{q})\delta(\mathbf{q})y_1 = \eta_1(\mathbf{q})\delta(\mathbf{q})y_2, \tag{5}$$

which can be viewed as the PTF from y_1 to y_2 given by

$$y_2 = \frac{\eta_2(\mathbf{q})\delta(\mathbf{q})}{\eta_1(\mathbf{q})\delta(\mathbf{q})}y_1. \tag{6}$$

Note that (6) is independent of the input u and could represent a transmissibility [6]. Hence identification is feasible despite lack of knowledge of the input u or its statistical properties. Because (6) is expressed in terms of the forward shift operator $\mathbf{q}$, (6) fully accounts for nonzero initial conditions. If we replace $\mathbf{q}$ with z in (6), the resulting relation would not account for nonzero initial conditions. A related approach, proposed in [7], does not consider IIR systems.

Furthermore, we note that (6) is a rational function in $\mathbf{q}$, an operator. Unlike a rational transfer function in z, a complex number, a common factor in $\mathbf{q}$ cannot generally be canceled from the numerator and denominator of (6), as illustrated by the following example.

Example 1.1: Consider the distinct sequences

$$y_1 = \{y_1(0), y_1(1), \ldots\} = \{1, 2, 3, \ldots\}, \tag{7}$$

$$y_2 = \{y_2(0), y_2(1), \ldots\} = \{6, 7, 8, \ldots\}. \tag{8}$$

Operating on (7) and (8) with $\mathbf{q}-1$, we obtain

$$(\mathbf{q}-1)y_1 = \{2-1, 3-2, 4-3, \ldots\} = \{1, 1, 1, \ldots\}, \tag{9}$$

$$(\mathbf{q}-1)y_2 = \{7-6, 8-7, 9-8, \ldots\} = \{1, 1, 1, \ldots\}. \tag{10}$$

Hence $(\mathbf{q}-1)y_1(k) = (\mathbf{q}-1)y_2(k)$, whereas $y_1 \neq y_2$.

Despite Example 1.1, we show that cancellation of the

Performed as a partnership under the auspices of the NASA Innovative Partnerships Program (IPP) under grant NNX08BA57A

[1]Ph.D. Student, University of Michigan, Ann Arbor, MI.
[2]Research Scientist, NASA Dryden.
[3]Professor, Dept. of Mechanical Eng., University of Michigan, Ann Arbor, MI.
[4]Professor, Dept. of Aerospace Eng., University of Michigan, Ann Arbor, MI 48109-2140, phone: (734) 764-3719, fax: (734) 763-0578, dsbaero@umich.edu.

978-1-4244-7425-7/10/$26.00 ©2010 AACC

common factor is permissible for PTFs. Consequently, $\delta(\mathbf{q})$ does not appear in the PTF from y_1 to y_2. However, some pole information contained in $\delta(\mathbf{q})$ is captured in the PTF through the effect of the system dynamics on the zeros, which are contained in $\eta_1(\mathbf{q})$ and $\eta_2(\mathbf{q})$.

To determine a PTF, output data are collected from sensors. As shown in Figure 1, one output (here sensor 1) is chosen to be the pseudo input while the other output (here sensor 2) is chosen to be the pseudo output. Then a system identification algorithm is used to identify the PTF from the pseudo input data y_1 to the pseudo output data y_2. We use Markov parameters to characterize the PTF because they exhibit consistency, that is, assuming $u(k)$ is white noise, the Markov parameters of the transfer function from u to y converge to their true values as the amount of data increases [8]. By comparing PTF estimates, we can detect a fault in the system if the PTF estimate changes.

II. INPUT-OUTPUT MODEL

Let $A \in \mathbb{R}^{n\times n}$, $B \in \mathbb{R}^{n\times m}$, $C \in \mathbb{R}^{p\times n}$, and $D \in \mathbb{R}^{p\times m}$, and consider the discrete-time MIMO LTI system

$$x(k+1)=Ax(k)+Bu(k), \quad y(k)=Cx(k)+Du(k), \tag{11}$$

where

$$u(k)\triangleq[u_1(k) \cdots u_m(k)]^{\mathrm{T}}, \quad y(k)\triangleq[y_1(k) \cdots y_p(k)]^{\mathrm{T}}. \tag{12}$$

We also write

$$y_i(k) = C_i x(k) + D_i u(k), \tag{13}$$

where, for $i \in \{1,\dots,p\}$, $C_i \in \mathbb{R}^{1\times n}$ and $D_i \in \mathbb{R}^{1\times m}$,

$$C\triangleq\begin{bmatrix} C_1^{\mathrm{T}} & \cdots & C_p^{\mathrm{T}} \end{bmatrix}^{\mathrm{T}}, \quad D\triangleq\begin{bmatrix} D_1^{\mathrm{T}} & \cdots & D_p^{\mathrm{T}} \end{bmatrix}^{\mathrm{T}}. \tag{14}$$

We rewrite (13) in terms of $\mathbf{q}$ as

$$\delta(\mathbf{q})y_i = N_i(\mathbf{q})u, \tag{15}$$

where

$$\delta(\mathbf{q}) \triangleq \det(\mathbf{q}I - A), \tag{16}$$

$$N_i(\mathbf{q}) \triangleq \begin{bmatrix} \eta_{i,1}(\mathbf{q}) & \cdots & \eta_{i,m}(\mathbf{q}) \end{bmatrix}, \tag{17}$$

$$\eta_{i,j}(\mathbf{q}) \triangleq C_i \mathrm{adj}(\mathbf{q}I - A)B_j + D_{i,j}\delta(\mathbf{q}), \tag{18}$$

adj$(\cdot)$ denotes the *adjugate* operator, and, for $B_i \in \mathbb{R}^n$ and $D_{i,j} \in \mathbb{R}$,

$$B\triangleq\begin{bmatrix} B_1 & \cdots & B_m \end{bmatrix}, \quad D_i\triangleq\begin{bmatrix} D_{i,1} & \cdots & D_{i,m} \end{bmatrix}. \tag{19}$$

Assuming $p \ge m$, we can write

$$\delta(\mathbf{q})\begin{bmatrix} y_1 & \cdots & y_m \end{bmatrix}^{\mathrm{T}} = E(\mathbf{q})u, \tag{20}$$

where

$$E(\mathbf{q}) \triangleq \begin{bmatrix} N_1^{\mathrm{T}}(\mathbf{q}) & \cdots & N_m^{\mathrm{T}}(\mathbf{q}) \end{bmatrix}^{\mathrm{T}} \in \mathbb{R}^{m\times m}. \tag{21}$$

III. OUTPUT-ONLY MODEL FOR $p \ge m$

Assuming $E(\mathbf{q})$ is invertible, we multiply (20) on the left by $E^{-1}(\mathbf{q})$ to obtain

$$\delta(\mathbf{q})E^{-1}(\mathbf{q})\begin{bmatrix} y_1 & \cdots & y_m \end{bmatrix}^{\mathrm{T}} = u. \tag{22}$$

Next, we note that

$$\delta(\mathbf{q})y_{m+1}=N_{m+1}(\mathbf{q})u. \tag{23}$$

Then, we multiply (22) on the left by $N_{m+1}(\mathbf{q})$ to obtain

$$\delta(\mathbf{q})N_{m+1}(\mathbf{q})E^{-1}(\mathbf{q})\begin{bmatrix} y_1 & \cdots & y_m \end{bmatrix}^{\mathrm{T}}=N_{m+1}(\mathbf{q})u. \tag{24}$$

Comparing (23) and (24), we see

$$y_{m+1} = \frac{\delta(\mathbf{q})N_{m+1}(\mathbf{q})E^{-1}(\mathbf{q})}{\delta(\mathbf{q})}\begin{bmatrix} y_1 & \cdots & y_m \end{bmatrix}^{\mathrm{T}}, \tag{25}$$

which can be interpreted as a multi-input, single-output PTF from $\begin{bmatrix} y_1 & \cdots & y_m \end{bmatrix}^{\mathrm{T}}$ to y_{m+1}.

IV. TWO-SENSOR, SINGLE-INPUT CASE

For $m = 1, p = 2$, we let $\eta_i(\mathbf{q}) = \eta_{i,1}(\mathbf{q})$ so that (25) reduces to (6). For $i = \{1,2\}$ we formulate an equivalent matrix representation of (6) by writing

$$\eta_i(\mathbf{q})=\textstyle\sum_{j=0}^{n} \beta_{i,j}\mathbf{q}^{n-j}, \quad \delta(\mathbf{q})=\mathbf{q}^n+\sum_{j=1}^{n} \alpha_j\mathbf{q}^{n-j}. \tag{26}$$

The following result shows that sampling a continuous-time transfer function $G(s)$ yields a discrete-time transfer function $G_h(q)$ whose relative degree is $d = 1$.

Fact 4.1: Let G be a continuous-time system with relative degree d. Then the relative degree of the discretized system G_h is 1, where h is the sampling period. Furthermore, as $h \to 0$, $d-1$ zeros of G_h approach the roots of $J_d(z)$, where

$$J_d(z) \triangleq J_{d,1}z^{d-1} + J_{d,2}z^{d-2} + \cdots + J_{d,d}, \tag{27}$$

and, for $i = 1,\dots,d$,

$$J_{d,i} \triangleq \sum_{\gamma=1}^{i}(-1)^{i-\gamma}\gamma^d \begin{pmatrix} d+1 \\ i-\gamma \end{pmatrix}. \tag{28}$$

Proof: See [9], Theorem 1. ■

Numerical results suggest that the roots of $B_d(z)$ are real for all $h > 0$.

Fact 4.2: Consider the continuous-time system

$$\dot{x}(t)=A_c x(t)+B_c u(t), \quad y(t)=Cx(t)+Du(t), \tag{29}$$

discretized using a zero-order hold to obtain

$$x(k+1)=e^{A_c T}x(k)+A_c^{-1}(A-I)B_c u(k), \; y(k)=Cx(k)+Du(k), \tag{30}$$

where T is the sampling period, and

$$\left(\mathbf{q}^n + \sum_{i=1}^{n}\alpha_i\mathbf{q}^{n-i}\right)y = \left(\sum_{i=0}^{n}\beta_i\mathbf{q}^{n-i}\right)u. \tag{31}$$

Then $\beta_1 \neq 0$.

Proof: The result follows from Fact 4.1. ■

We then express (6) as

$$\Delta v=0, \tag{32}$$

where, for $l > 2n$ data points, we define

$$\Delta \triangleq \begin{bmatrix} \alpha_n & \dots & \alpha_1 & 1 & 0 & \dots & 0 \\ 0 & \alpha_n & \dots & \alpha_1 & 1 & \ddots & \vdots \\ \vdots & \ddots & \ddots & \ddots & \ddots & \ddots & 0 \\ 0 & \dots & 0 & \alpha_n & \dots & \alpha_1 & 1 \end{bmatrix} \in \mathbb{R}^{(l-2n)\times(l-n)}. \tag{33}$$

Furthermore,

$$v = NY \in \mathbb{R}^{l-n}, \tag{34}$$

where

$$N \triangleq \begin{bmatrix} N_2 & -N_1 \end{bmatrix} \in \mathbb{R}^{(l-n)\times 2l}, \tag{35}$$

and for $i \in \{1,2\}$,

$$N_i \triangleq \begin{bmatrix} \beta_{i,n} & \dots & \beta_{i,0} & 0 & \dots & 0 \\ 0 & \beta_{i,n} & \dots & \beta_{i,0} & \ddots & \vdots \\ \vdots & \ddots & \ddots & \ddots & \ddots & 0 \\ 0 & \dots & 0 & \beta_{i,n} & \dots & \beta_{i,0} \end{bmatrix} \in \mathbb{R}^{(l-n)\times l}. \tag{36}$$

Finally, we define

$$Y \triangleq \begin{bmatrix} Y_1^{\mathrm{T}} \; Y_2^{\mathrm{T}} \end{bmatrix}^{\mathrm{T}} \triangleq [y_1(0) \cdots y_1(l-1) \; y_2(0) \cdots y_2(l-1)]^{\mathrm{T}} \in \mathbb{R}^{2l}. \tag{37}$$

Combining (32) and (34) yields

$$\Delta NY = 0, \tag{38}$$

which is an equivalent matrix formulation of (6).

For $i = \{1,2\}$, from (11) and (13) we have [10, p. 129]

$$Y_i = \Gamma_i x_0 + \mathcal{H}_i U, \tag{39}$$

where

$$\Gamma_i \triangleq \begin{bmatrix} C_i \\ \vdots \\ C_i A^{l-1} \end{bmatrix} \in \mathbb{R}^{l\times n}, \quad U \triangleq \begin{bmatrix} u(0) \\ \vdots \\ u(l-1) \end{bmatrix} \in \mathbb{R}^{l}$$

$$\mathcal{H}_i \triangleq \begin{bmatrix} D_i & 0 & \dots & 0 \\ C_i B & D_i & \ddots & \vdots \\ \vdots & \ddots & \ddots & 0 \\ C_i A^{l-2} B & \dots & C_i B & D_i \end{bmatrix}$$

$$\triangleq \begin{bmatrix} H_{i,0} & 0 & \dots & 0 \\ H_{i,1} & H_{i,0} & \ddots & \vdots \\ \vdots & \ddots & \ddots & \vdots \\ H_{i,l-1} & \dots & \dots & H_{i,0} \end{bmatrix} \in \mathbb{R}^{l\times l}. \tag{40}$$

Then we define

$$Y_{i,\text{free}} \triangleq \Gamma_i x_0, \quad Y_{i,\text{forced}} \triangleq \mathcal{H}_i U, \tag{41}$$

so that

$$Y_i = Y_{i,\text{free}} + Y_{i,\text{forced}}. \tag{42}$$

Furthermore,

$$Y = \Gamma x_0 + \mathcal{H} U, \tag{43}$$

where

$$\Gamma \triangleq \begin{bmatrix} \Gamma_1^{\mathrm{T}} & \Gamma_2^{\mathrm{T}} \end{bmatrix}^{\mathrm{T}}, \quad \mathcal{H} \triangleq \begin{bmatrix} \mathcal{H}_1^{\mathrm{T}} & \mathcal{H}_2^{\mathrm{T}} \end{bmatrix}^{\mathrm{T}}. \tag{44}$$

Finally,

$$Y = Y_{\text{free}} + Y_{\text{forced}}, \tag{45}$$

where

$$Y_{\text{free}} \triangleq \begin{bmatrix} Y_{1,\text{free}}^{\mathrm{T}} \; Y_{2,\text{free}}^{\mathrm{T}} \end{bmatrix}^{\mathrm{T}}, \quad Y_{\text{forced}} \triangleq \begin{bmatrix} Y_{1,\text{forced}}^{\mathrm{T}} \; Y_{2,\text{forced}}^{\mathrm{T}} \end{bmatrix}^{\mathrm{T}}. \tag{46}$$

Hence, (38) can be written as

$$\Delta N(Y_{\text{free}} + Y_{\text{forced}}) = 0. \tag{47}$$

Lemma 4.3: $N_2\Gamma_1 = N_1\Gamma_2$.

Proof: Assume $l > 2n$. Then

$$N_2\Gamma_1 = \begin{bmatrix} \sum_{i=0}^{n} \beta_{2,i} C_1 A^i \\ \vdots \\ \sum_{i=0}^{n} \beta_{2,i} C_1 A^{l-n-1+i} \end{bmatrix}, \tag{48}$$

$$N_1\Gamma_2 = \begin{bmatrix} \sum_{i=0}^{n} \beta_{1,i} C_2 A^i \\ \vdots \\ \sum_{i=0}^{n} \beta_{1,i} C_2 A^{l-n-1+i} \end{bmatrix}. \tag{49}$$

Using (65), it follows that the first component of (48) and the first component of (49) are identical. Furthermore, multiplying (65) on the right by A^{q-1} implies that, for $q \in \{2,3,\dots,l-n\}$, the q^{th} component of (48) and the q^{th} component of (49) are also identical. ■

Proposition 4.4: $NY_{\text{free}} = 0$.

Proof: With $u(k) \equiv 0$, (39) implies

$$N_2 Y_{1,\text{free}} = N_2\Gamma_1 x(0), \tag{50}$$

$$N_1 Y_{2,\text{free}} = N_1\Gamma_2 x(0). \tag{51}$$

Subtracting (51) from (50) and invoking Lemma 4.3, we have

$$\begin{aligned} NY_{\text{free}} &= N_2 Y_{1,\text{free}} - N_1 Y_{2,\text{free}} \\ &= N_2\Gamma_1 x(0) - N_1\Gamma_2 x(0) = 0. \end{aligned}$$ ■

Lemma 4.5: $N_2\mathcal{H}_1 = N_1\mathcal{H}_2$.

Proof: Assume $l > 2n$. Then

$$N_2\mathcal{H}_1 = \begin{bmatrix} \sigma_{2,1}(1,1) & \dots & \sigma_{2,1}(1,n+1) & 0 & 0 \\ \vdots & \ddots & \ddots & \ddots & \vdots \\ \sigma_{2,1}(l-n,1) & \dots & \sigma_{2,1}(1,1) & \dots & \sigma_{2,1}(1,n+1) \end{bmatrix},$$

$$N_1\mathcal{H}_2 = \begin{bmatrix} \sigma_{1,2}(1,1) & \dots & \sigma_{1,2}(1,n+1) & 0 & 0 \\ \vdots & \ddots & \ddots & \ddots & \vdots \\ \sigma_{1,2}(l-n,1) & \dots & \sigma_{1,2}(1,1) & \dots & \sigma_{1,2}(1,n+1) \end{bmatrix},$$

are Toeplitz and

$$\sigma_{j,k}(r,s) \triangleq \sum_{i=s-1}^{n} \beta_{j,n-i} H_{k,i+r-s}.$$

For $q \in \{0,1,\dots,l-n-2\}$, multiplying (65) on the right by $A^q B$ implies that, for $r \in \{2,3,\dots,l-n\}$,

$$\sigma_{2,1}(r,1) = \sigma_{1,2}(r,1).$$

Furthermore, setting $k = s-1$ in (66) implies that, for $s \in \{1,2,\dots,n+1\}$,

$$\sigma_{2,1}(1,s) = \sigma_{1,2}(1,s).$$ ■

Proposition 4.6: $NY_{\text{forced}} = 0$.

Proof: With $x_0 = 0$, (39) implies

$$N_2 Y_{1,\text{forced}} = N_2\mathcal{H}_1 U, \tag{52}$$

$$N_1 Y_{2,\text{forced}} = N_1\mathcal{H}_2 U. \tag{53}$$

Subtracting (53) from (52) and invoking Lemma 4.5 yields

$$NY_{\text{forced}} = N_2 Y_{1,\text{forced}} - N_1 Y_{2,\text{forced}}$$
$$= N_2 \mathcal{H}_1 U - N_1 \mathcal{H}_2 U = 0. \qquad \blacksquare$$

Propositions 4.4 and 4.6 yield the following result, which is stronger than (38).

Theorem 4.7: $NY = 0$.

We note that Theorem 4.7 is an equivalent matrix formulation of

$$y_2 = \frac{\eta_2(\mathbf{q})}{\eta_1(\mathbf{q})} y_1. \tag{54}$$

Comparing (54) with (6), we see Theorem 4.7 implies cancellation of the $\delta(\mathbf{q})$ in the numerator and denominator of (6) is valid. The following result implies that PTFs are always causal.

Fact 4.8: Assume the PTF in (54) is obtained by sampling a continuous time system using zero-order hold. Then the PTF has order $n-1$ and relative degree 0.

Proof: From Fact 4.2, it follows that $\eta_1(\mathbf{q})$ and $\eta_2(\mathbf{q})$ have degree $n-1$. $\blacksquare$

V. THREE-SENSOR, TWO-INPUT CASE

Let $p = 3$ and $m = 1$. Then the PTF from y_1 to y_3 is given by (25) as

$$y_3 = \frac{\delta(\mathbf{q})\eta_{3,1}(\mathbf{q})}{\delta(\mathbf{q})\eta_{1,1}(\mathbf{q})} y_1. \tag{55}$$

Next, let $m = 2$. Then the PTF from $[y_1\ y_2]^{\mathrm{T}}$ to y_3 is

$$\delta(\mathbf{q})\,[\eta_{3,1}(\mathbf{q})\ \eta_{3,2}(\mathbf{q})] \begin{bmatrix} \eta_{1,1}(\mathbf{q}) & \eta_{1,2}(\mathbf{q}) \\ \eta_{2,1}(\mathbf{q}) & \eta_{2,2}(\mathbf{q}) \end{bmatrix}^{-1} [y_1\ y_2]^{\mathrm{T}} = \delta(\mathbf{q}) y_3, \tag{56}$$

which implies

$$y_3 = \frac{\delta(\mathbf{q})\,[\eta_{3,1}(\mathbf{q})\eta_{2,2}(\mathbf{q}) - \eta_{3,2}(\mathbf{q})\eta_{2,1}(\mathbf{q})]}{\delta(\mathbf{q})\,[\eta_{1,1}(\mathbf{q})\eta_{2,2}(\mathbf{q}) - \eta_{2,1}(\mathbf{q})\eta_{1,2}(\mathbf{q})]} y_1 + \frac{\delta(\mathbf{q})\,[\eta_{3,2}(\mathbf{q})\eta_{1,1}(\mathbf{q}) - \eta_{3,1}(\mathbf{q})\eta_{1,2}(\mathbf{q})]}{\delta(\mathbf{q})\,[\eta_{1,1}(\mathbf{q})\eta_{2,2}(\mathbf{q}) - \eta_{2,1}(\mathbf{q})\eta_{1,2}(\mathbf{q})]} y_2. \tag{57}$$

Therefore, the SISO PTF from y_1 to y_3 given by (55) does not equal the corresponding component of the MISO PTF given by (57). This implies physically that the location and number of inputs affect the PTF, even though the statistical characteristics of the input do not.

VI. SINGLE INPUT EXAMPLES

Consider the mass-spring-damper structure in Figure 2, which has equations of motion given by

$$M\ddot{x} + C\dot{x} + Kx = F, \tag{58}$$

where

$$x = \begin{bmatrix} q_1 \\ q_2 \end{bmatrix},\ M = \begin{bmatrix} m_1 & 0 \\ 0 & m_2 \end{bmatrix},\ C = \begin{bmatrix} c_1 + c_2 & -c_2 \\ -c_2 & c_2 + c_3 \end{bmatrix},$$
$$K = \begin{bmatrix} k_1 + k_2 & -k_2 \\ -k_2 & k_2 + k_3 \end{bmatrix},\ F = \begin{bmatrix} f_1 \\ f_2 \end{bmatrix} = \begin{bmatrix} 1 \\ 0 \end{bmatrix} u. \tag{59}$$

We derive the numerically exact PTF from q_1 to q_2 by discretizing (58) and (59).

A. Square-Wave Input, $x_0 \neq 0$

We choose $\{x_i(0)\}_{i=1}^4 \sim N(0,1)$ and $\{u(k)\}_{k=0}^{49}$ to be a square wave with amplitude 1 and frequency $1/2\pi$. We then simulate (58)–(59) to obtain $\{q_1(k)\}_{k=0}^{49}$ and $\{q_2(k)\}_{k=0}^{49}$. Next, we use standard least squares to estimate the first 3 Markov parameters of the PTF from q_1 to q_2 and compare the estimated Markov parameters with their true values in Figure 3, which shows that the estimated Markov parameters approach their true values for sufficiently large l.

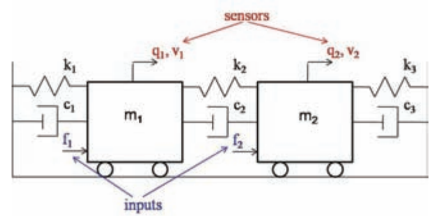

Fig. 2. 2 DOF Mass-spring-damper structure.

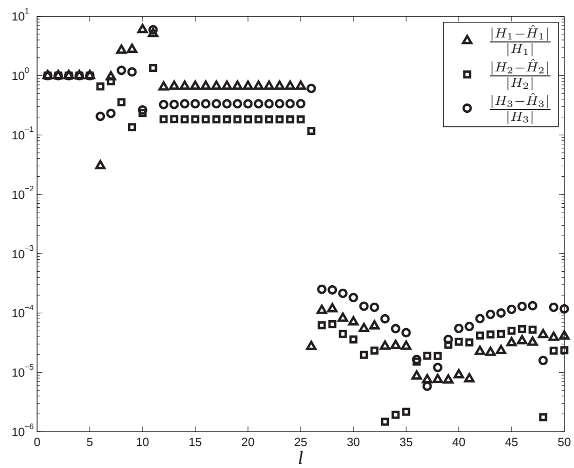

Fig. 3. Numerical simulation with unknown nonzero initial conditions. $u(k)$ is a square wave with amplitude 1 and frequency $1/2\pi$, and $\{x_i(0)\}_{i=1}^4 \sim N(0,1)$. The error between the estimated and true Markov parameters is small, but bias is present in the estimate.

B. Sum of Sinusoids Input, $x_0 \neq 0$

We choose $\{x_i(0)\}_{i=1}^4 \sim N(0,1)$ and $\{u(k)\}_{k=0}^{49}$ to be a sine wave with amplitude 1 and frequency 0.25 Hz added to a sine wave with amplitude 1 and frequency 0.5. We then simulate (58) and (59) to obtain $\{q_1(k)\}_{k=0}^{49}$ and $\{q_2(k)\}_{k=0}^{49}$. Next, we use standard least squares to estimate the first 3 Markov parameters of the PTF from q_1 to q_2 and compare the estimated Markov parameters with their true values in Figure 4, which shows that the estimated Markov parameters approach their true values for sufficiently large l.

C. Parameter Change Detection - White Noise Input, $x_0 \neq 0$

We investigate whether changes in PTFs can be used to detect changes in system parameters. We choose $\{x_i(0)\}_{i=1}^4 \sim N(0,1)$ and $\{u(k)\}_{k=0}^{99} \sim N(0,1)$ and simulate (58)–(59) to obtain $\{q_1(k)\}_{k=0}^{99}$ and $\{q_2(k)\}_{k=0}^{99}$. At $k = 49$, the stiffness k_i are reduced by a factor of 2 and the damping c_i are increased by a factor of 3. From Figure 5 we observe an abrupt increase in Markov parameter error at $k = 50$. Since we use recursive least squares in this example with a forgetting factor of 0.7, we see the Markov parameter estimates converge to their new values after damage occurs.

D. Effect of Sensor Noise on PTF Identification

We investigate the effect of sensor noise on the accuracy of the identified PTF by considering noise added to the pseudo

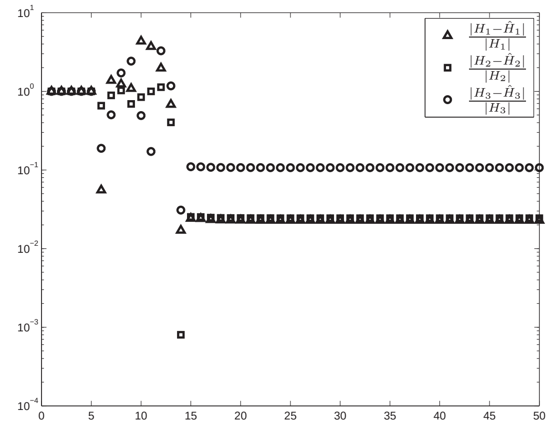

Fig. 4. Numerical simulation with $\{x_i(0)\}_{i=1}^4 \sim N(0,1)$. The input is a sum of two sinusoids with amplitude 1 and frequencies 0.25 Hz and 0.5 Hz. The error between the estimated and true Markov parameters is small, but bias is present in the estimate.

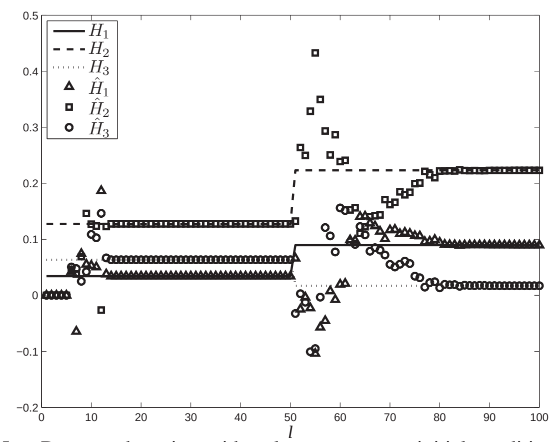

Fig. 5. Damage detection with unknown nonzero initial conditions. The input is $\{u(k)\}_{k=0}^{99} \sim N(0,1)$, $\{x_i(0)\}_{i=1}^4 \sim N(0,1)$, and damage occurs at 5 seconds. The identified Markov parameters approach their true values both before and after damage occurs.

output and pseudo input. We quantify the difference between the estimated and actual Markov parameters by defining

$$\varepsilon_{\mathcal{T}_\mu} \triangleq \sigma_{\max}\left(\mathcal{T}_\mu - \hat{\mathcal{T}_\mu}\right), \tag{60}$$

where

$$\mathcal{T}_\mu \triangleq \begin{bmatrix} H_0 & \cdots & 0 \\ \vdots & \ddots & 0 \\ H_{\mu-1} & \cdots & H_0 \end{bmatrix} \tag{61}$$

is the truncated Toeplitz operator [8]. We choose $\{x_i(0)\}_{i=1}^4 \sim N(0,1)$ and $\{u(k)\}_{k=0}^{l-1} \sim N(0,1)$ and simulate (58)–(59) to obtain $\{q_1(k)\}_{k=0}^{l-1}$ and $\{q_2(k)\}_{k=0}^{l-1}$. We also choose 100 Gaussian white noise sequences $\{w(k)\}_{k=0}^{l-1}$. Using a $\mu-$Markov model structure [8], we assume the PTF is order 3 and estimate the first $\mu = 10$ Markov parameters of the PTF from y_1 to y_2 for each noise sequence. For pseudo output noise, we choose $y_1 = \{q_1(k)\}_{k=0}^{l-1}$ and $y_2 = \{q_2(k) + w(k)\}_{k=0}^{l-1}$. We use the estimated and true Markov parameters to compute $\varepsilon_{\mathcal{T}_\mu}$, which we average over all noise sequences by computing $\bar{\varepsilon}_{\mathcal{T}_\mu} = \frac{1}{100}\sum_{j=1}^{100} \varepsilon_{\mathcal{T}_{\mu_j}}$. For pseudo input noise, we instead compute the estimated Markov parameters for each white noise sequence using $y_1 = \{q_1(k) + w(k)\}_{k=0}^{l-1}$ and $y_2 = \{q_2(k)\}_{k=0}^{l-1}$.

Figure 6 shows that $\bar{\varepsilon}_{\mathcal{T}_\mu}$ decreases as SNR and l increase for sensor noise added to the pseudo output and pseudo input. For large SNR, Figure 6 shows that PTF Markov parameter estimates in the presence of pseudo input noise are more accurate than estimates in the presence of pseudo output noise, which implies that noisier sensors should be chosen as pseudo inputs. For a given SNR, Figure 6 shows that $\bar{\varepsilon}_{\mathcal{T}_\mu}$ does not decrease monotonically with l, which implies that PTF Markov parameter estimates are not consistent.

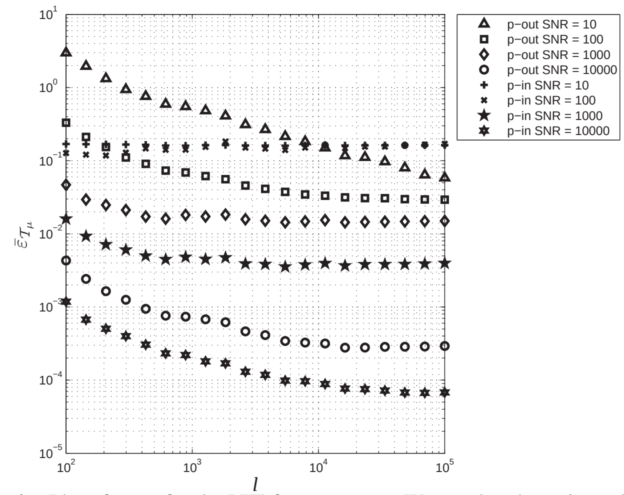

Fig. 6. Plot of $\bar{\varepsilon}_{\mathcal{T}_{10}}$ for the PTF from q_1 to q_2. We see that the estimated Markov parameters approach their true values as the SNR and l increase, but the estimation is not consistent. For large SNR, we see that estimation in the presence of pseudo input noise is more accurate than estimation in the presence of pseudo output noise.

VII. MULTIPLE INPUT EXAMPLES

We consider the two-input case for the 2-DOF system given by (58). Then we have

$$F = \begin{bmatrix} 1 & 0 \\ 0 & 1 \end{bmatrix} \begin{bmatrix} u_1 \\ u_2 \end{bmatrix}. \tag{62}$$

We choose $\{x_i(0)\}_{i=1}^4 \sim N(0,1)$, $\{u_1(k)\}_{k=0}^{99} \sim N(0,1)$, and $\{u_2(k)\}_{k=0}^{99} \sim N(0,1)$. We then simulate (58)–(59) to obtain $\{q_1(k)\}_{k=0}^{99}$ and $\{q_2(k)\}_{k=0}^{99}$. Next, we compare the estimated and exact Markov parameters of the PTF from q_1 to q_2 in Figure 7. We see from Figure 7 that the estimated and exact Markov parameters do not match no matter how much data is included in the regressor. Therefore, a PTF with a single pseudo input cannot characterize the simulated 2-DOF system with 2 inputs. To characterize a system with m inputs, the PTF must have m pseudo inputs. As evidence, we investigate a 3-DOF system with 2 inputs.

Consider the mass-spring-damper structure shown in Fig-

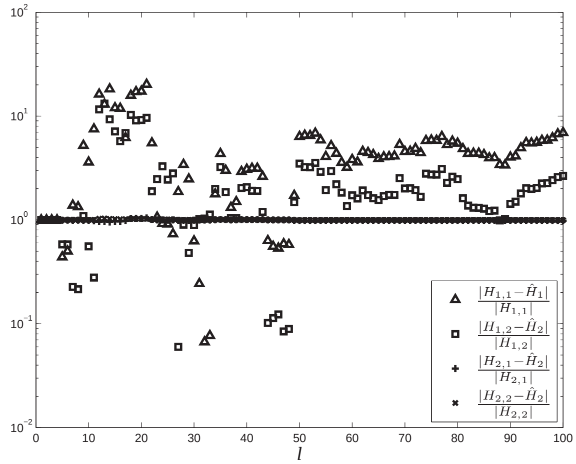

Fig. 7. PTF identification for $m = 2$ using 1 pseudo input. The inputs are $\{u_1(k)\}_{k=0}^{99} \sim N(0,1)$ and $\{u_2(k)\}_{k=0}^{99} \sim N(0,1)$, and $\{x_i(0)\}_{i=1}^{4} \sim N(0,1)$. Since the Markov parameter error does not decrease with l, a PTF with 1 pseudo input does not properly characterize a system with $m > 1$.

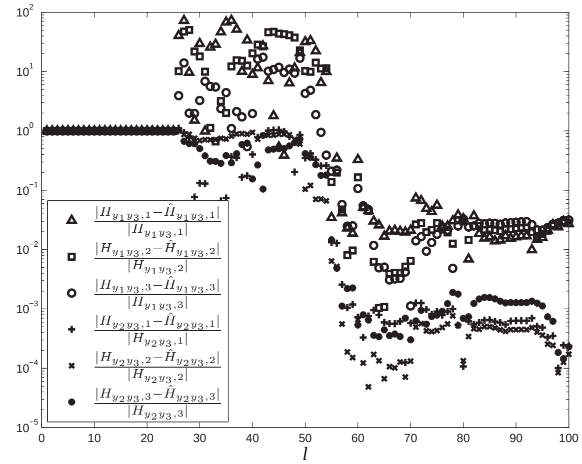

Fig. 9. PTF identification for $m = 2$ using 2 pseudo inputs. The inputs are $\{u_1(k)\}_{k=0}^{99} \sim N(0,1)$ and $\{u_2(k)\}_{k=0}^{99} \sim N(0,1)$, and $\{x_i(0)\}_{i=1}^{6} \sim N(0,1)$. Because the Markov parameter error decreases with l, a PTF with 2 pseudo inputs can characterize a system with $m = 2$.

ure 8, which has equations of motion given by (58), where

$$x = \begin{bmatrix} q_1 \\ q_2 \\ q_3 \end{bmatrix}, M = \begin{bmatrix} m_1 & 0 & 0 \\ 0 & m_2 & 0 \\ 0 & 0 & m_3 \end{bmatrix}, F = \begin{bmatrix} f_1 \\ f_2 \\ f_3 \end{bmatrix} = \begin{bmatrix} 1 & 0 \\ 0 & 1 \\ 0 & 0 \end{bmatrix} u,$$

$$C = \begin{bmatrix} c_1 + c_2 & -c_2 & 0 \\ -c_2 & c_2 + c_3 & -c_3 \\ 0 & -c_3 & c_3 + c_4 \end{bmatrix},$$

$$K = \begin{bmatrix} k_1 + k_2 & -k_2 & 0 \\ -k_2 & k_2 + k_3 & -k_3 \\ 0 & -k_3 & k_3 + k_4 \end{bmatrix}. \quad (63)$$

We derive the numerically exact PTF from $[q_1 \quad q_2]^{\mathrm{T}}$ to q_3 by discretizing (58) and (63).

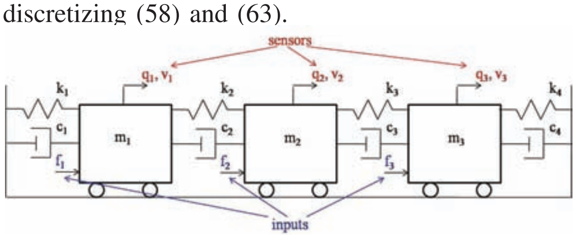

Fig. 8. 3 DOF Mass-spring-damper structure.

A. White Input ($m = 2$), $x_0 \neq 0$

We choose $\{x_i(0)\}_{i=1}^{6} \sim N(0,1)$, $\{u_1(k)\}_{k=0}^{99} \sim N(0,1)$, and $\{u_2(k)\}_{k=0}^{99} \sim N(0,1)$. We then simulate (58) with (63) to obtain $\{q_1(k)\}_{k=0}^{99}$, $\{q_2(k)\}_{k=0}^{99}$, and $\{q_3(k)\}_{k=0}^{99}$. The error between the estimated and exact Markov parameters of the PTF from $[q_1 \quad q_2]^{\mathrm{T}}$ to q_3 is plotted in Figure 9, which shows the PTF with two pseudo inputs is identified for the 3-DOF system with $m = 2$.

VIII. APPENDICES

Let $A \in \mathbb{R}^{n\times n}, B \in \mathbb{R}^{n\times 1}, C_1, C_2 \in \mathbb{R}^{1\times n}$, $D_1, D_2 \in \mathbb{R}$, $r = \{1, 2\}$, and

$$H_{r,i} \triangleq \begin{cases} D_r, & i = 0, \\ C_r A^{i-1} B, & else. \end{cases} \quad (64)$$

Then

$$\sum_{i=0}^{n} \beta_{2,n-i} C_1 A^i = \sum_{i=0}^{n} \beta_{1,n-i} C_2 A^i, \quad (65)$$

and for all $k \in \{0, 1, \ldots, n\}$,

$$\sum_{i=k}^{n} \beta_{2,n-i} H_{1,i-k} = \sum_{i=k}^{n} \beta_{1,n-i} H_{2,i-k}, \quad (66)$$

where $\beta_{r,j}$ are the coefficients of

$$\left(\mathbf{q}^n + \alpha_1 \mathbf{q}^{n-1} + \cdots + \alpha_n\right) y_r = \left(\beta_{r,0}\mathbf{q}^n + \beta_{r,1}\mathbf{q}^{n-1} + \cdots + \beta_{r,n}\right) u, \quad (67)$$

which corresponds to the discrete-time system

$$x(k+1) = Ax(k) + Bu(k), \quad y_r(k) = C_r x(k) + D_r u(k). \quad (68)$$

REFERENCES

[1] F. Poncelet, G. Kerschen, J.-C. Golinval, D. Verhelst, “Output-only modal analysis using blind source separation techniques,” *Mechanical Systems and Signal Processing*, Vol. 21, pp. 2335–2358, 2007.

[2] I. Bradaric, A.P. Petropulu, K.I. Diamantaras, “Blind MIMO FIR channel identification based on second-order spectra correlations,” *IEEE Trans. Sig. Processing*, Vol. 51, no. 6, pp. 1668–1674, 2003.

[3] L. Mevel, A. Benveniste, M. Basseville, M. Goursat, B. Peeters, H. Van der Auweraer, A. Vecchio,“Input/output versus output only data processing for structural identification–application to in-flight data analysis,” *Journal of Sound & Vibration*, Vol. 295, pp. 531–552, 2006.

[4] A. Deraemaeker, E. Reynders, G. De Roeck. J. Kullaa, “Vibration-based structural health monitoring using output-only measurements under changing environment,” *Mechanical Systems and Signal Processing*, Vol. 22, pp. 34–56, 2008.

[5] A. M. D’Amato, A. J. Brzezinski, M. S. Holzel, J. Ni, D. S. Bernstein, “Sensor-only noncausal blind identification of pseudo transfer functions,” *Proc. SYSID*, pp. 1698–1703, Saint-Malo, France, July 2009.

[6] C. Rainieri, G. Fabbrocino, “Automated output-only dynamic identification of civil engineering structures,” *Mechanical Systems and Signal Processing*, doi: 10:1016/j.ymssp.2009.10.003, 2009.

[7] G. Xu, H. Liu, L. Tong, T. Kailath, “A least-squares approach to blind channel identification,” *IEEE Trans. Sig. Proc.*, Vol. 43, no. 12, 1995.

[8] M. S. Fledderjohn, M. S. Holzel, H. J. Palanthandalam-Madapusi, R. J. Fuentes, and D. S. Bernstein, “A comparison of least squares algorithms for estimating Markov parameters”, *Proc. Amer. Contr. Conf.*, Baltimore, MD, June 2010.

[9] K.J. Astrom, P. Hagander, J. Sternby, “Zeros of sampled systems,” *Automatica*, Vol. 20, no. 1, pp. 31–38, 1984.

[10] J. S. Bay, *Fundamentals of Linear State Space Systems*, 1998.